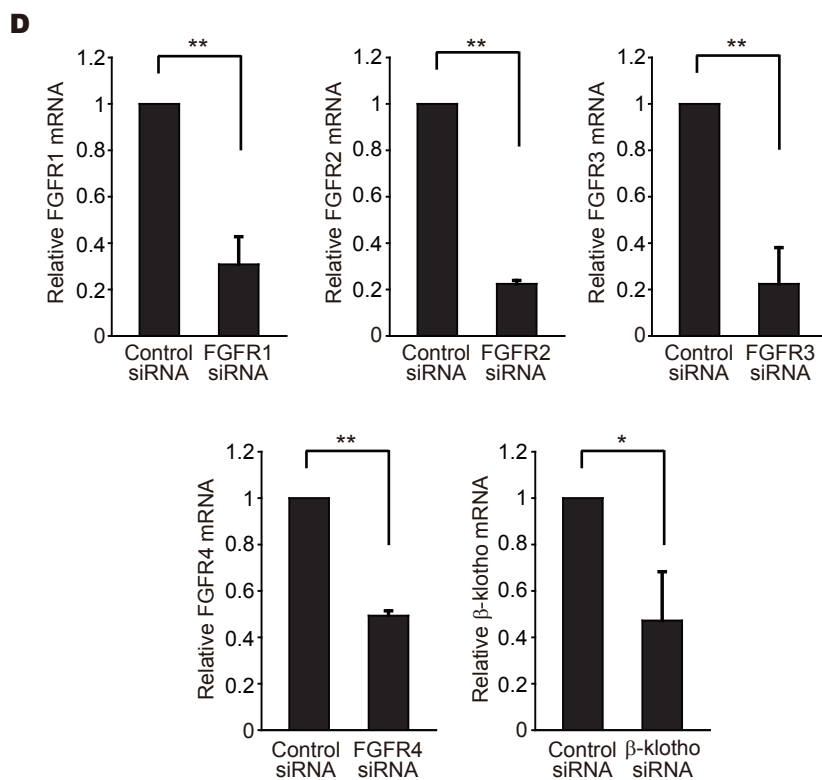
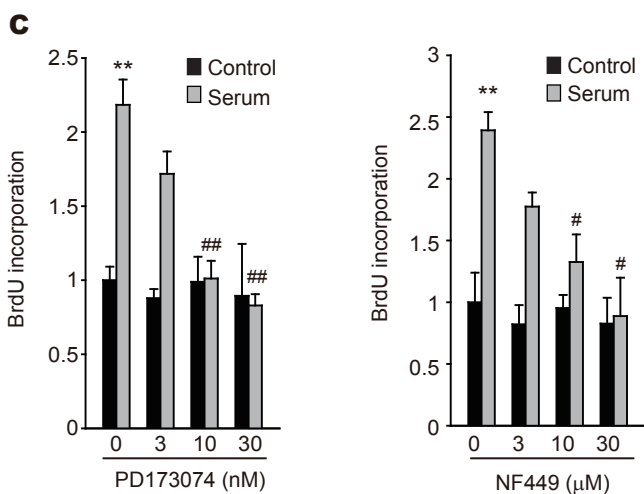
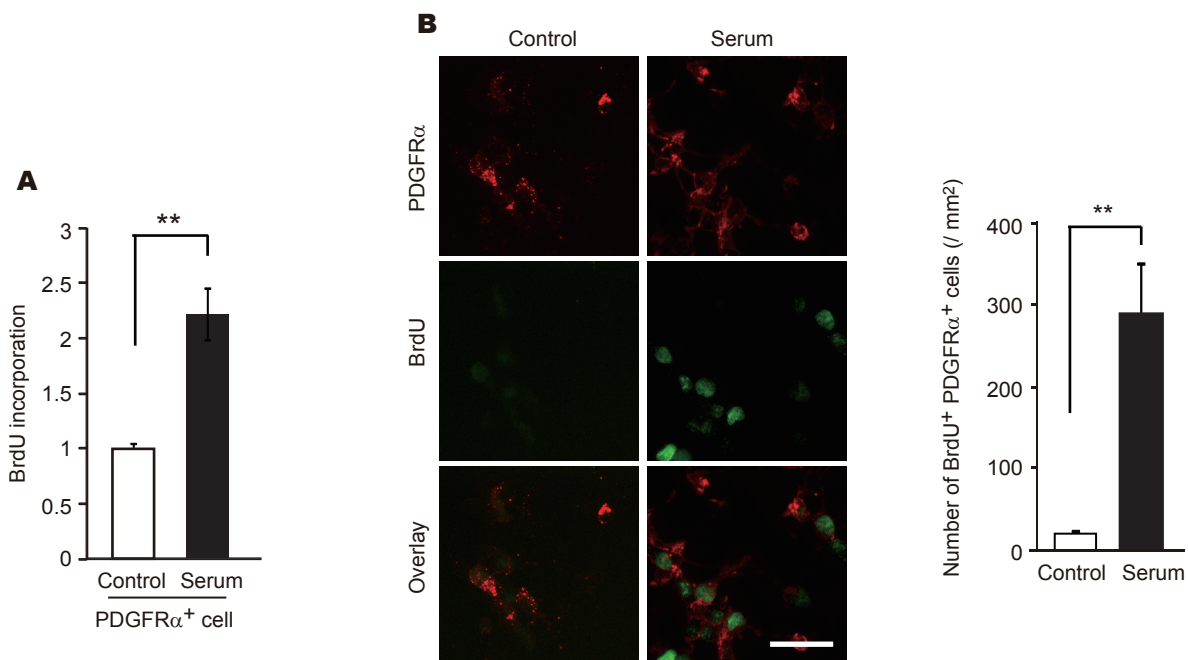


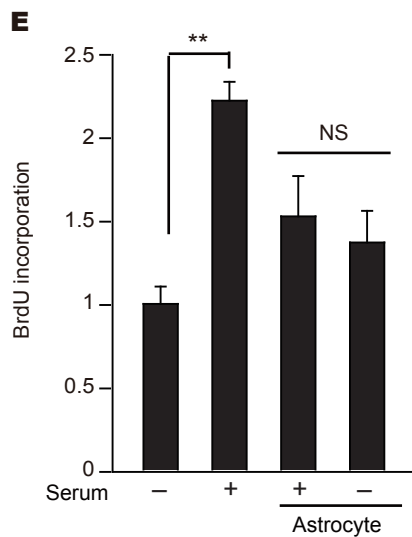
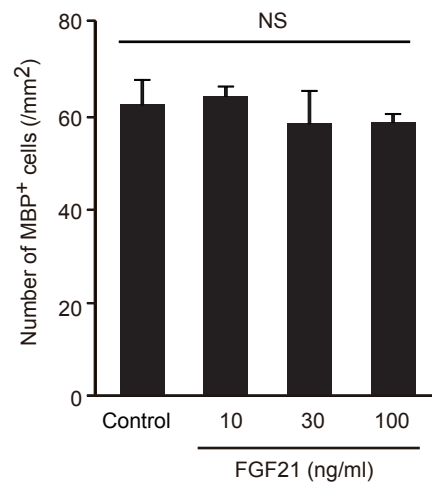
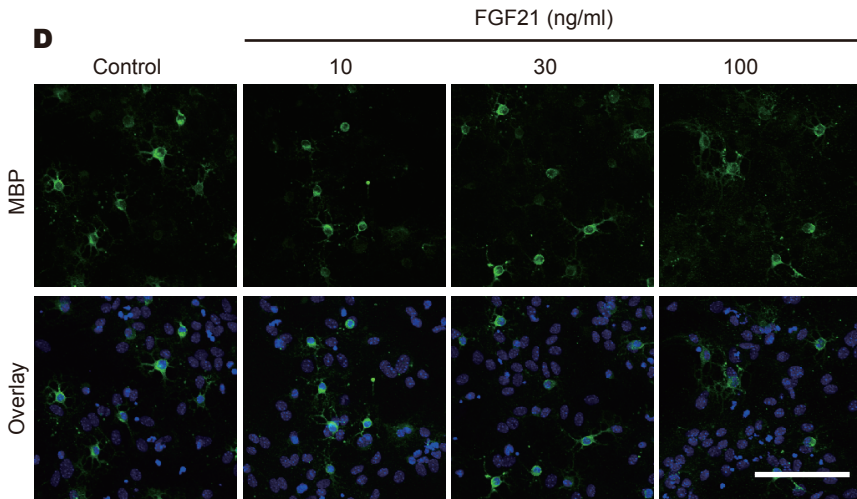
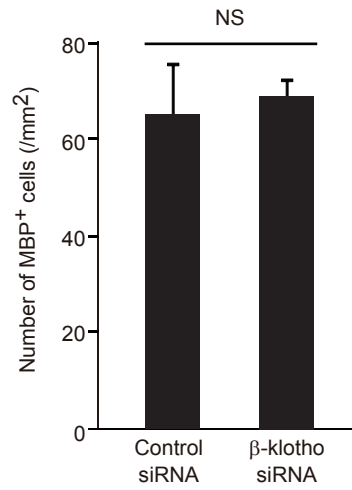
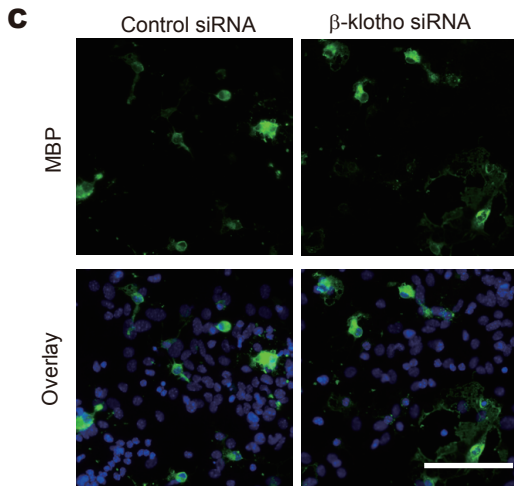
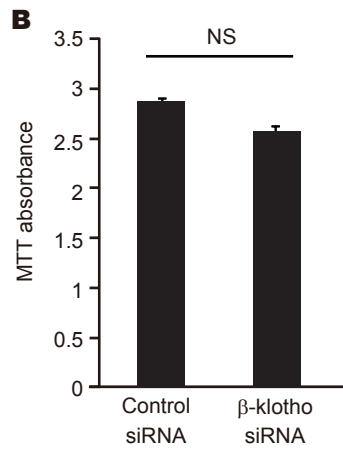
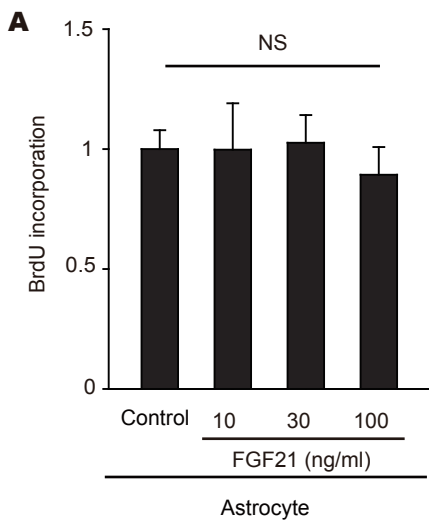
Supplemental Figure 1 Time course of vascular barrier disruption and remyelination.

(A) Representative image of spinal cord sections labeled with NeuN. Sections were prepared 3 days after LPC injection. Graph show NeuN⁺ cell density in the spinal cord section (n= 4 for Control, n= 6 for LPC); $P = 0.70913$. (B) Representative images of spinal cord sections visualized with MBP (upper panel) and endogenous IgG (lower panel). Sections were prepared 3 days after saline injection. (C) Representative images of brain sections visualized with MBP (upper panel) and endogenous IgG (lower panel) the indicated number of days after removal of the cuprizone diet. Graphs show the time course of demyelination the indicated number of days after removal of the cuprizone diet (n = 3 each); $P = 0.0017$ as determined by Student's *t*-test or ANOVA with Tukey's test. Error bars represent s.e.m. NS indicates no significant difference. Scale bars: 100 μm for A and B, 50 μm for C.



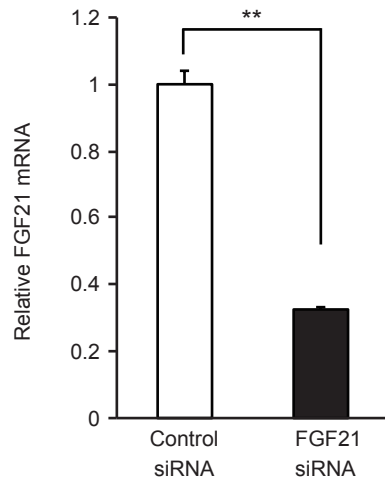
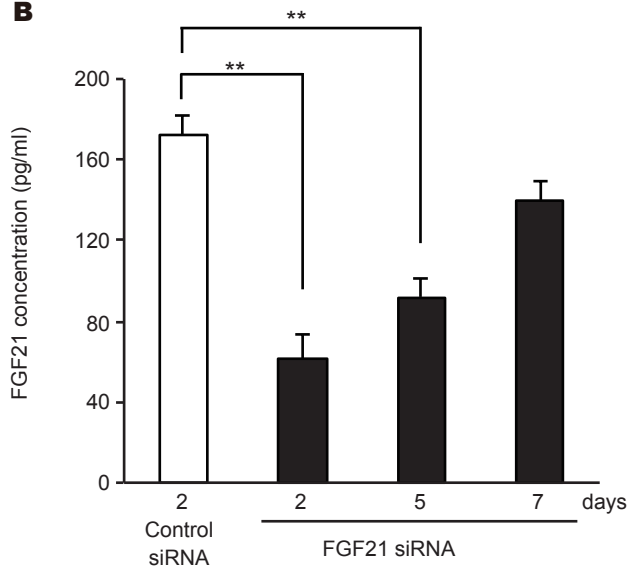
Supplemental Figure 2 FGF21 signaling is involved in circulating factor–mediated OPC proliferation.

(A) Concentration-dependence of BrdU incorporation in PDGFR α ⁺ OPCs cultured with adult mouse serum (n = 6); $P < 0.0001$. (B) Representative images of OPC culture isolated using A2B5-positive microbeads. Cells were cultured with adult mouse serum, and then double-labeled for PDGFR α and BrdU. No cells that were double-labeled for GFAP and BrdU were detected in the culture. Graphs show quantitation as indicated in each images. (n = 9); $P < 0.0001$. (C) BrdU incorporation in OPCs after serum stimulation with PD173074 (left, n = 4) and NF449 (right, n = 4); $P < 0.0001$ (left graph), $P = 0.0009, 0.0231, 0.0013$ (right graph, left to right). #, ## compared with serum treatment. (D) Relative expression of FGFRs mRNA in OPCs after transfection with siRNAs against the indicated FGFRs. A2B5⁺ cells were isolated 48 h after transfection (n = 3 for FGFR1, n = 4 for FGFR2, n = 5 for FGFR3, n = 3 for FGFR4, n = 4 for β -klotho); $P = 0.0022, 0.0001, 0.001, 0.0001, 0.023$ (left to right) as determined by Student's t-test, ANOVA with Tukey's post-hoc test. Error bars represent s.e.m. NS indicates not significant. Scale bars: 50 μ m.



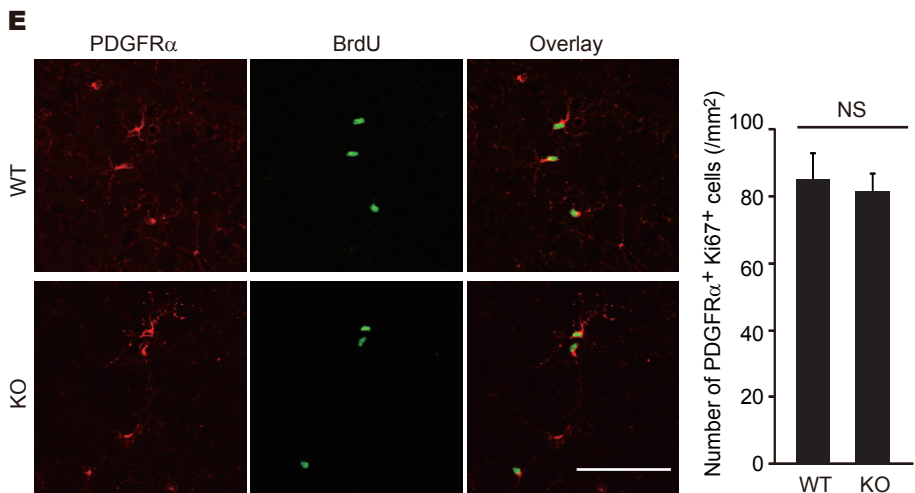
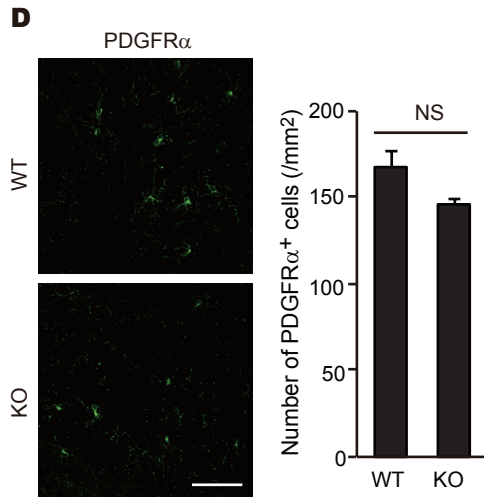
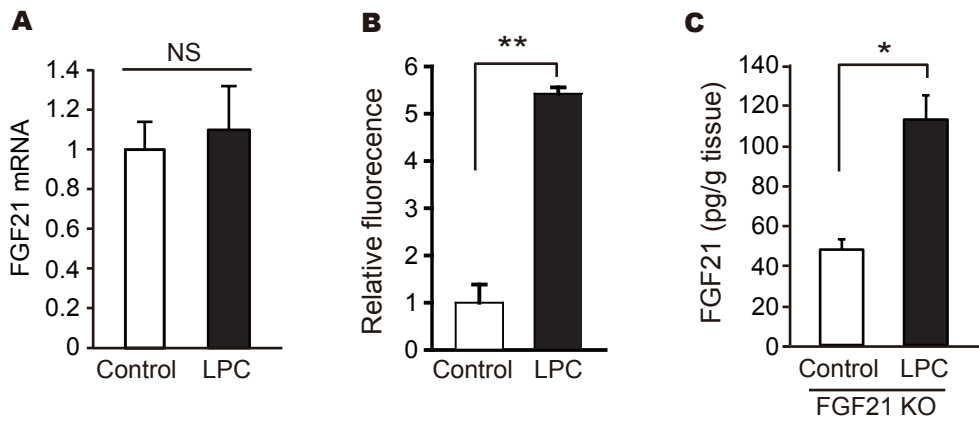
Supplemental Figure 3 Astrocyte is not involved in FGF21-mediated OPC proliferation.

(A) BrdU incorporation in astrocyte 3 days after stimulation with the indicated concentrations of FGF21 (n = 4), $P = 0.8956$. (B) Change in MTT reduction in OPCs 48 h after β -klotho siRNA transfection (n = 6); $P = 0.7936$. (C) Representative images of cultures labeled for MBP and DAPI. OPCs were transfected with β -klotho siRNA. Graphs show quantitation as indicated in each image (n = 4); $P = 0.4044$. (D) Representative images of culture labeled for MBP and DAPI. OPCs were treated with recombinant FGF21. Graphs show quantitation as indicated in each images (n = 3); $P = 0.9321, 0.6148, 0.6744$ (left to right). (E) BrdU incorporation in A2B5⁺ OPCs 3 days after stimulation with astrocyte supernatant. Astrocytes were cultured for 1 day with or without stimulation with adult mouse serum. After culture, the astrocyte supernatant was collected and added into the A2B5⁺ cell culture (n = 6); $P = 0.0002$ as determined by Student's *t*-test, ANOVA with Tukey's post-hoc test. Error bars represent s.e.m. NS indicates not significant. Scale bars: 50 μ m.

A**B**

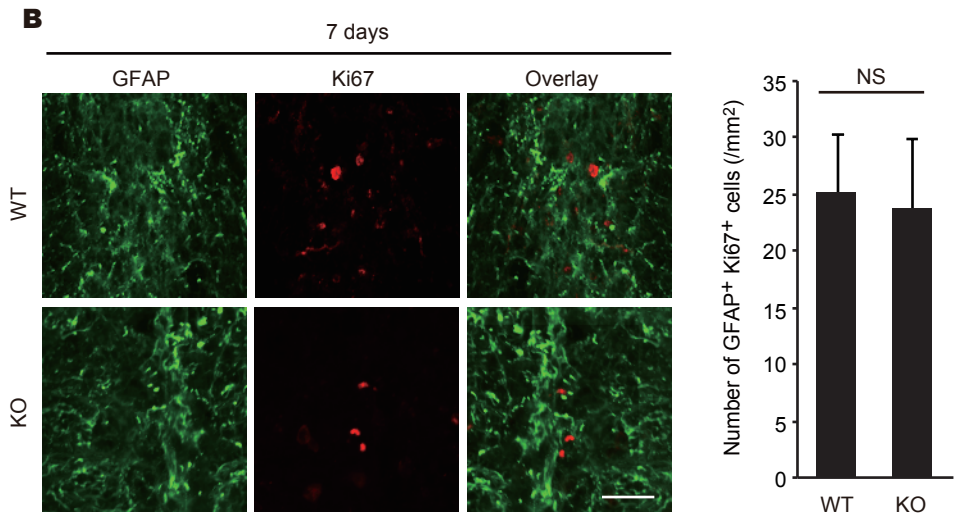
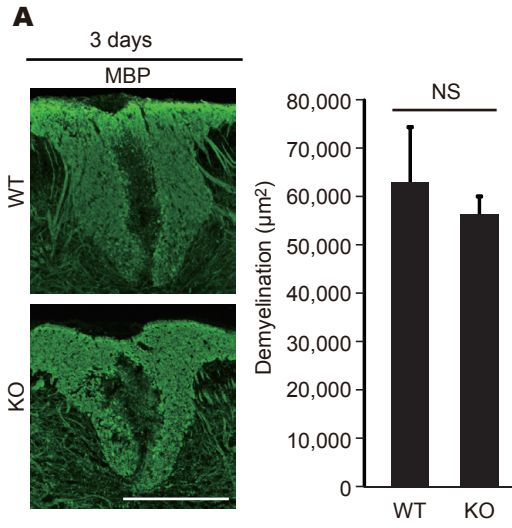
Supplemental Figure 4 FGF21 in the CNS from the circulation.

(A) Relative expression of FGF21 mRNA in pancreas 2 days after siRNA transfection (n = 3); $P = 0.0001$. (B) FGF21 content in serum of mice that received FGF21 siRNA transfection (n = 3 for control siRNA, 5 for other groups). Serum was prepared the indicated number of days after siRNA injection; $P = 0.0004, 0.0047$ (left to right) as determined by Student's *t*-test or ANOVA with Dunnett's test. Error bars represent s.e.m.



Supplemental Figure 5 Peripheral Fgf21 promotes OPC proliferation and remyelination.

(A) Quantitations of *Fgf21* mRNA in the spinal cord 3 days after LPC injection ($n = 4$); $P = 0.0353$. NS indicates not significant. (B) Relative intensity of fluorescence in the spinal cord 3 days after LPC injection. WT mice intravenously received recombinant FGF21 which is labeled with HiLyte Fluor 555 ($n = 3$); $P = 0.004$. (C) Measurement of FGF21 in spinal cord (pg/g) of *Fgf21*-knockout mice ($n = 3$) infused subcutaneously with FGF21 for 7 days; $P = 0.0191$. (D) Representative images of spinal cord sections labeled for PDGFR α . Spinal cord sections were obtained from *Fgf21*-knockout mice and control littermates. Graphs show quantitations as indicated in the images ($n = 4$); $P = 0.1091$. NS indicates not significant. (E) Representative images of spinal cord sections double-labeled for PDGFR α and BrdU. Spinal cord sections were obtained from *Fgf21*-knockout mice and control littermates. Graphs show quantitations as indicated in the images ($n = 3$); $P = 0.7953$. (F) Representative images of spinal cord sections labeled for MBP. Spinal cord sections were obtained from *Fgf21*-knockout mice and control littermates. Graphs show quantitations as indicated in the images ($n = 4$); $P = 0.5106$ as determined by Student's *t*-test. Error bars represent s.e.m. NS indicates not significant. Scale bars: 50 μm for D and E, 200 μm for F.

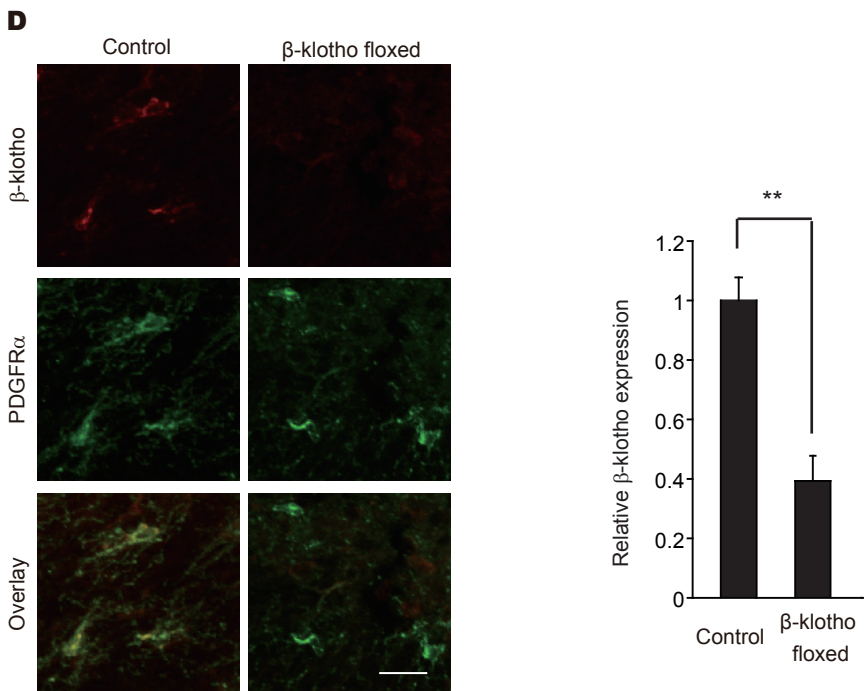
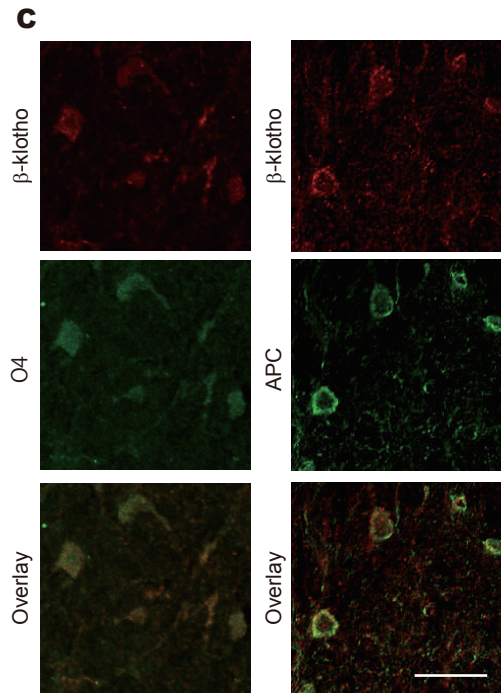
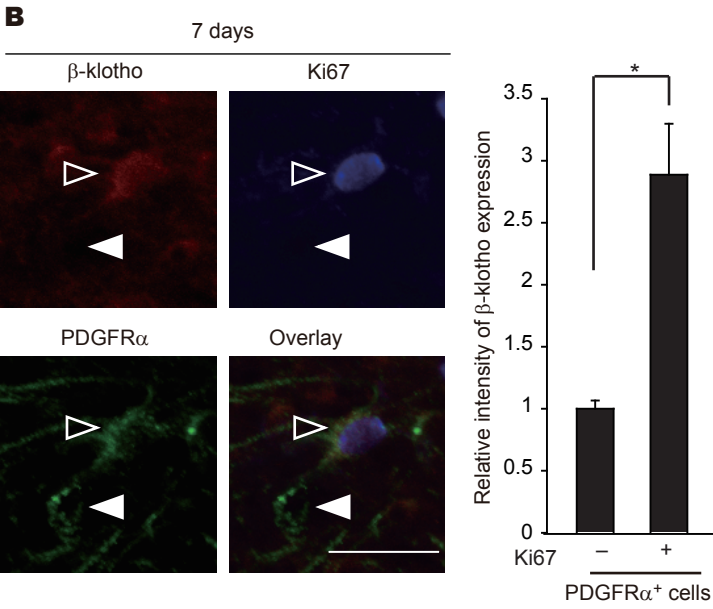
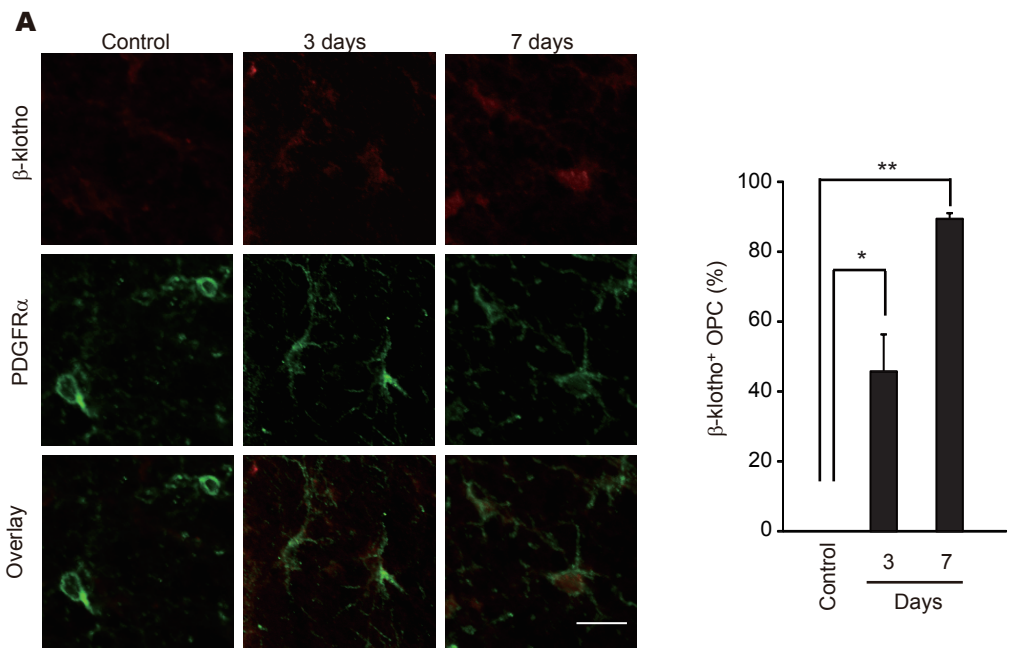


Supplemental Figure 6 Peripheral Fgf21 does not associate with demyelination.

(A) Representative images of spinal cord sections labeled for MBP 3 days after LPC injection. Spinal cord sections were obtained from *Fgf21*-knockout mice and control littermates. Graphs show quantitations as indicated in the images (n = 3); $P = 0.45144$.

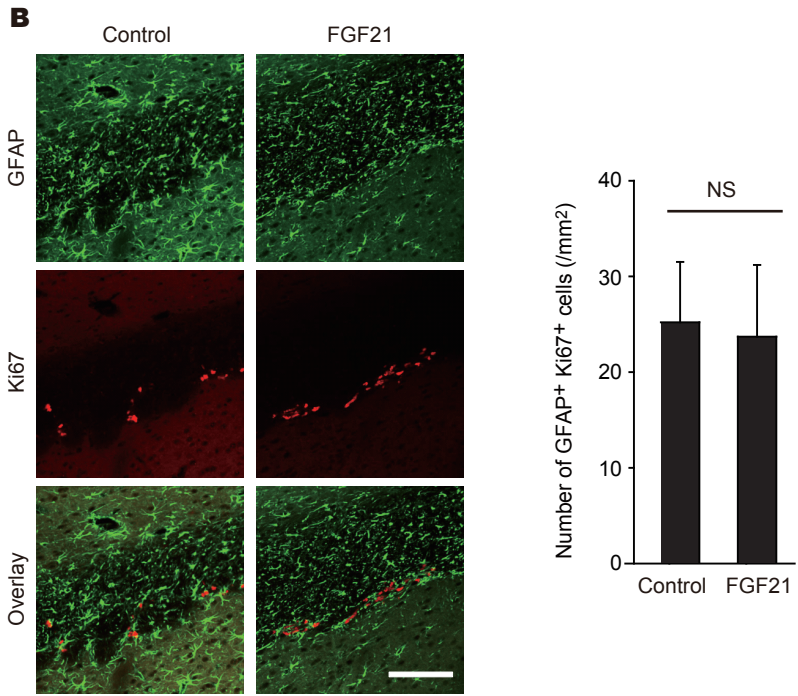
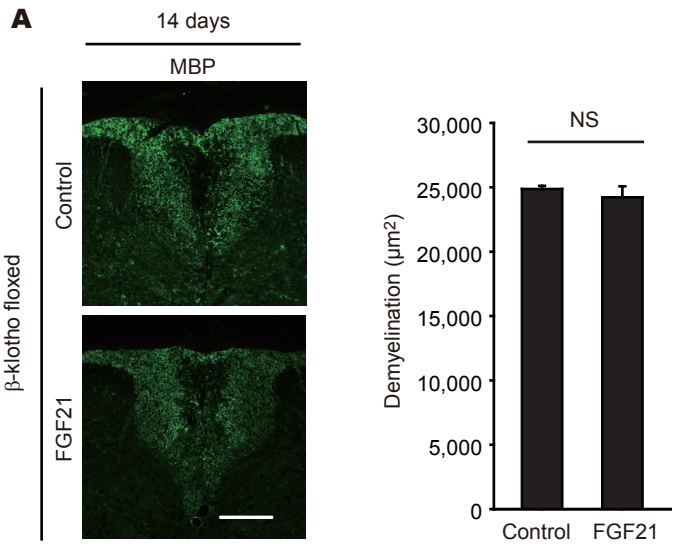
(B) Representative images of spinal cord sections labeled for GFAP 7 days after LPC injection. Spinal cord sections were obtained from *Fgf21*-knockout mice and control littermates. Graphs show quantitations as indicated in the images (n = 3); $P = 0.8851$ as determined by Student's *t*-test. Error bars represent s.e.m. NS indicates not significant.

Scale bars: 200 μm for **A**, 50 μm for **B**.



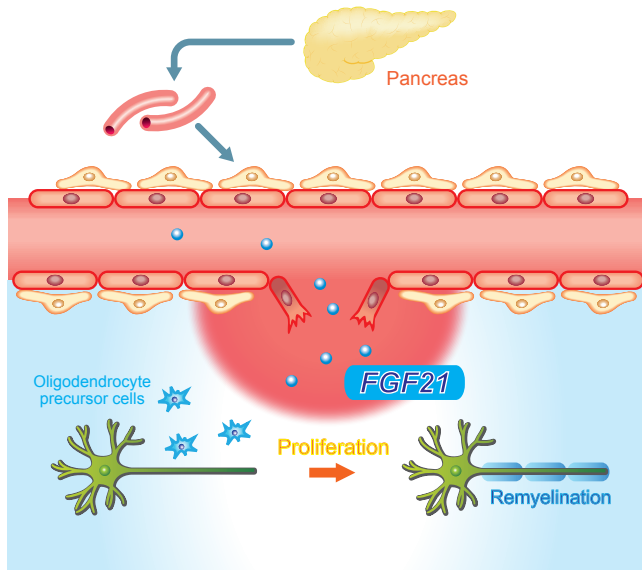
Supplemental Figure 7 β -klotho expression is involved in OPC proliferation after demyelination.

(A) Representative images of spinal cord sections double-labeled for PDGFR α and β -klotho. Graphs show quantitation as indicated in the images ($n = 3$); $P = 0.0145$, 0.0005 (left to right). (B) Representative images of spinal cord sections triple-labeled for PDGFR α , Ki67, and β -klotho. Spinal cord sections were obtained 7 days after LPC injection. Graphs show quantitation as indicated in the images ($n = 3$); $P = 0.011$. Open arrowhead indicates a Ki67-positive cell labeled with PDGFR α . White arrowhead indicates a Ki67-negative cell labeled with PDGFR α . (C) Representative image of spinal cord sections double-labeled for O4 (left) or APC (right) with β -klotho. Spinal cords were obtained 3 days after LPC injection. (D) Relative intensity of β -klotho protein expression in PDGFR α -positive OPCs obtained from spinal cords of β -klotho-conditional knockout mice 7 days after LPC injection ($n = 3$ each); $P = 0.0062$ as determined by Student's t -test or ANOVA with Dunnett's test. Error bars represent s.e.m. NS indicates not significant. Scale bars: 20 μm for A, B and D, 50 μm for C.



Supplemental Figure 8 β -klotho expression in OPC is essential for remyelination by peripheral hormone.

(A) Representative images of spinal cord sections labeled for MBP. Spinal cord sections were obtained from β -klotho-conditional knockout mice with or without FGF21 treatment. Graphs show quantitations as indicated in the images (n = 4); $P = 0.4997$. (B) Representative images of brain sections double-labeled for GFAP and Ki67. Brain sections were obtained 7 days after injury. Graphs show quantitations as indicated in the images (n = 3); $P = 0.8851$ as determined by Student's *t*-test. Error bars represent s.e.m. NS indicates not significant. Scale bars: 20 μ m for 200 μ m for **A**, 100 μ m for **B**.



Supplemental Figure 9 Diagrammatic illustration of this study.

CNS is isolated from peripheral milieu by the vascular barrier. Therefore, CNS regeneration has been thought to be controlled by the CNS microenvironment *in situ*. However, CNS injury disrupts the vascular barrier, leading to leakage of circulating factors into the CNS. One of these factors, FGF21 expressed in pancreas, promotes OPC proliferation and subsequent remyelination. We propose that peripheral milieu regulates CNS regeneration.

Inhibitor	Inhibition rate (%)	Inhibitor	Inhibition rate (%)
ATM Kinase	118.33	JNK Inhibitor II	49.98
ATM/ ATR Kinase Inhibitor	-51.37	JAK3 Inhibitor IV	-20.49
AG 1024	94.95	JNK Inhibitor, Negative Control	-10.53
AG L 2043	135.01	IGF-1R Inhibitor II	-40.63
Akt Inhibitor IV	-27.87	JNK Inhibitor V	-22.59
Akt Inhibitor V, Triciribine	127.38	JNK Inhibitor VIII	90.00
Akt Inhibitor VIII, Isozyme-Selective,	-27.53	K-252a, Nocardioopsis sp.	-21.99
Akt Inhibitor X	-52.15	KN-93	-21.09
Aminopurvalanol A	131.09	Lck Inhibitor	-21.96
AMPK Inhibitor, Compound C	134.93	LY 294002	8.32
Aurora Kinase Inhibitor II	117.20	LY 303511- Negative control	117.54
Aurora Kinase Inhibitor III	116.92	MEK Inhibitor I	-12.97
Aurora Kinase/Cdk Inhibitor	112.71	MEK Inhibitor II	121.32
BAY11-7082	134.01	MEK1/2 Inhibitor	37.69
Bcr-abl Inhibitor	2.25	MNK1 Inhibitor	29.47
Bisindolylmaleimide I	135.82	MK2a Inhibitor	-0.45
Bisindolylmaleimide IV	119.54	NF449	26.31
Bohemine	148.06	NF-kB Activation Inhibitor	-6.45
BPIQ-I	117.06	p38 MAP Kinase Inhibitor III	-13.76
Cdk1 Inhibitor	133.30	p38 MAP Kinase Inhibitor	29.46
Cdk1 Inhibitor, CGP74514A	82.28	PD 98059	52.55
Cdk1/2 Inhibitor III	79.87	PD 169316	12.03
Cdk1/5 Inhibitor	93.16	PD 158780	8.99
Casein Kinase I Inhibitor, D4476	109.62	PD 173074	19.49
Casein Kinase II Inhibitor III, TBCA	101.96	PD 174265	-16.49
Cdk4 Inhibitor II, NSC 625987	102.37	PDGF Receptor Tyrosine Kinase	-73.53
Cdk4 Inhibitor III	-21.85	PDGF Receptor Tyrosine Kinase	-24.1
Cdc2-Like Kinase Inhibitor, TG003	100.06	PDGF RTK Inhibitor	-67.15
Cdk/Crk Inhibitor	95.33	PDK1/Akt/Fli Dual Pathway Inhibitor	-31.40
Chelerythrine Chloride	-38.82	PKR Inhibitor	-85.61
Chk2 Inhibitor II	73.83	PKR Inhibitor, Negative Control	-28.16
Compound 52	127.38	PI-103	-68.06
Compound 56	105.07	PI 3-Kg Inhibitor	53.20
Cdk2 Inhibitor III	133.70	PI 3-Kg Inhibitor II	19.57
Cdk2 Inhibitor IV, NU6140	-18.97	SB 218078	-34.31
DNA-PK Inhibitor II	95.87	SC-68376	131.22
DNA-PK Inhibitor III	87.55	SKF-86002	56.82
DNA-PK Inhibitor V	88.99	Sphingosine Kinase Inhibitor	-32.77
Diacylglycerol Kinase Inhibitor II	-36.30	Src Kinase Inhibitor I	-51.58
DMBI	96.66	Staurosporine, Streptomyces sp.	-33.01
EGFR Inhibitor	-38.06	STO-609	133.24
EGFR/ErbB-2/ErbB-4 Inhibitor	152.83	SU6656	84.14
ERK Inhibitor II, FR180204	105.79	SU9516	37.45
ERK Inhibitor II, Negative control	125.28	SU 11652	-32.69
ERK Inhibitor III	95.03	Syk Inhibitor	110.96
Fascaplysin, Synthetic	-32.44	Syk Inhibitor II	40.63
Flt-3 Inhibitor	108.46	Syk Inhibitor III	91.39
Flt-3 Inhibitor II	104.42	Tpl2 Kinase Inhibitor	123.67
Flt-3 Inhibitor III	87.06	TGF-b RI Kinase Inhibitor	68.65
GSK-3b Inhibitor I	-44.49	TGF-b RI Inhibitor III	-28.28
GSK-3b Inhibitor II	103.53	AG 9	63.04
GSK-3b Inhibitor VIII	150.74	AG 490	-27.77
GSK-3b Inhibitor XI	175.07	AG 112	89.44
GSK3b Inhibitor XII, TWS 119	156.94	AG 1295	96.15
GSK-3 Inhibitor XIII	191.45	AG 1296	63.69
Gö 6983	111.18	AG 1478	64.42
GTP-14564	107.52	VEGF Receptor 2 Kinase Inhibitor I	59.23
Isogranulatimide	121.86	VEGF Receptor Tyrosine Kinase	30.61
H-89, Dihydrochloride	105.79	VEGFR Tyrosine Kinase Inhibitor IV	-24.64
H A 1077, Dihydrochloride	113.76	VEGF Receptor 2 Kinase Inhibitor II	95.16
Herbimycin A, Streptomyces sp.	56.24	VEGF Receptor 2 Kinase Inhibitor III	42.94
IC261	126.31	VEGF Receptor 2 Kinase Inhibitor IV	82.36
IKK-2 Inhibitor IV	124.55	Wortmannin	62.02
Indirubin Derivative E804	-40.71	ROCK Inhibitor, Y-27632	134.25
JAK3 Inhibitor II	120.53		

Supplemental Table 1 Pharmacological screening of BrdU incorporation into OPCs after serum treatment.

Inhibitors, except for PD173074 (10 nM), were used at a final concentration of 10 μ M.

Inhibition ratios of BrdU incorporation was calculated by the following formula:

Inhibition ratio = (Absorbance of the sample treated with serum and indicated inhibitor – Absorbance of the sample treated indicated inhibitor) / (Absorbance of the sample treated with serum – Absorbance of the control) \times 100. A lower value indicates more inhibition.